



Chinese Pharmaceutical Association
Institute of Materia Medica, Chinese Academy of Medical Sciences

Acta Pharmaceutica Sinica B

www.elsevier.com/locate/apsb
www.sciencedirect.com



ORIGINAL ARTICLE

Controlling tumor progression and recurrence in mice through combined treatment with a PD-L1 inhibitor and a designer *Salmonella* strain that delivers GM-CSF



Heung Jin Jeon^{a,†}, Daejin Lim^{b,†}, EunA So^c, Solbi Kim^d,
Jae-Ho Jeong^{c,*}, Miryoung Song^{e,*}, Hyo-Jin Lee^{a,d,f,*}

^aInfection Control Convergence Research Center, Chungnam National University College of Medicine, Daejeon 35015, Republic of Korea

^bDivision of Biomedical Convergence, College of Biomedical Science, Kangwon National University, Chuncheon 24341, Republic of Korea

^cDepartment of Microbiology, Chonnam National University Medical School, Gwangju 58128, Republic of Korea

^dDepartment of Medical Science, Chungnam National University College of Medicine, Daejeon 35015, Republic of Korea

^eDepartment of Bioscience and Biotechnology, Hankuk University of Foreign Studies, Yongin 17035, Republic of Korea

^fDepartment of Internal Medicine, Chungnam National University College of Medicine, Daejeon 35015, Republic of Korea

Received 1 March 2024; received in revised form 10 June 2024; accepted 28 June 2024

KEY WORDS

Checkpoint inhibitor;
Granulocyte macrophage
colony stimulating
factor;
Programmed death-ligand
1;
Salmonella

Abstract Combination therapy with checkpoint inhibitors blocks inhibitory immune cell signaling and improves clinical responses to anticancer treatments. However, continued development of innovative and controllable delivery systems for immune-stimulating agents is necessary to optimize clinical responses. Herein, we engineered *Salmonella* to deliver recombinant granulocyte macrophage colony stimulating factor (GM-CSF) in a controllable manner for combination treatment with a programmed death-ligand 1 (PD-L1) inhibitor. The engineered *Salmonella* enabled delivery of recombinant GM-CSF into mouse tumors, activating recruitment of immune cells, such as M1-polarized macrophages, dendritic cells, and CD8⁺ T cells. Combination treatment with the PD-L1 inhibitor and engineered *Salmonella* increased the survival rate of tumor-bearing mice by 25%. New tumor growth was strongly suppressed, and visible tumors disappeared at 120 days post-infection (dpi) in mice rechallenged with additional tumor

*Corresponding authors.

E-mail addresses: jeongjaeho@jnu.ac.kr (Jae-Ho Jeong), songm@hufs.ac.kr (Miryoung Song), cymed@cnu.ac.kr (Hyo-Jin Lee).

[†]These authors made equal contributions to this journal.

Peer review under the responsibility of Chinese Pharmaceutical Association and Institute of Materia Medica, Chinese Academy of Medical Sciences.

<https://doi.org/10.1016/j.apsb.2024.07.011>

2211-3835 © 2024 The Authors. Published by Elsevier B.V. on behalf of Chinese Pharmaceutical Association and Institute of Materia Medica, Chinese Academy of Medical Sciences. This is an open access article under the CC BY-NC-ND license (<http://creativecommons.org/licenses/by-nc-nd/4.0/>).

implantation at 100 dpi. The number of memory T cells increased >2-fold in tumor-rechallenged mice. Our findings demonstrate superiority of the engineered *Salmonella* as a cancer therapeutic agent with precise targeting ability, immune-boosting activity, and ease of combination with other therapeutics.

© 2024 The Authors. Published by Elsevier B.V. on behalf of Chinese Pharmaceutical Association and Institute of Materia Medica, Chinese Academy of Medical Sciences. This is an open access article under the CC BY-NC-ND license (<http://creativecommons.org/licenses/by-nc-nd/4.0/>).

1. Introduction

The aim of cancer therapy is to cure or inhibit the growth of cancer to stop disease progression. Various treatment modalities are used, including surgery, radiation therapy, chemotherapy, targeted therapy, and immunotherapy. Although such treatments can save lives, cancer remains a leading cause of death worldwide, and researchers are pursuing new treatment options for a complete cure with no side effects. Bacteria-mediated cancer therapy was originally developed based on observed tumor regression in patients with bacterial infections¹. The clinical use of attenuated *Mycobacterium bovis* (Bacillus Calmette–Guerin) has been approved by the US Food and Drug Administration (FDA) as an immunotherapeutic treatment for high-risk patients with non-muscle invasive bladder cancer². Naturally, certain bacteria, such as *Salmonella*, preferentially colonize the tumor microenvironment (TME), resulting in tumor regression³. Previous studies using animal models, have shown that *Salmonella* strains carrying therapeutic payloads (including immune modulators, angiogenesis modulators, prodrug-converting enzymes, short-interfering RNAs, and cytotoxic agents) can attenuate tumor growth and extend survival^{4–7}. To optimize therapeutic effects, payloads should be delivered in a controllable manner to expand the pool of therapeutic effectors.

Bacterial flagella are supramolecular nanomachines that enable motility and adhesion to host tissues. Many layers of regulation control the expression of components required for the proper formation of flagellum substructures, which are composed of a basal body embedded in an envelope, a hook, and a filament^{8–10}. The components of the hook and filament are translocated through the flagellar type-3 secretion system (T3SS), where each protein moves along the channel of the growing structure and assembles at the end^{10,11}. The master regulator FlhDC controls the genetic expression of structural proteins in the hook-basal body (HBB) and filament cap, as well as other regulatory proteins (including FlgM), by binding to the promoters of the FlhD₄C₂ complex^{8,12}. Once FlgM is expressed, it binds to FliA, a flagella-specific sigma factor (σ^{28}), to form the FliA–FlgM complex, which inhibits the transcription of genes encoding motor, filament, and chemotactic proteins¹³. When a functional HBB assembles, the sigma factor and anti-sigma factor complex (FliA–FlgM complex) interact with the export apparatus, after which FlgM is secreted. This leads to the activation of transcriptionally inhibited genes in the absence of FliA. FlgM secretion through the flagellar T3SS is directed by signal sequences at the N-terminus, where the secretion efficiency can be controlled by binding of the cognate chaperone, FliA, to the C-terminus. Previous results showed that FlgM can serve as a secretion tag for a recombinant protein, where the heterologous

protein with an N-terminal FlgM tag was expressed in the cytoplasm of *Escherichia coli* and exported via the flagellar T3SS^{14,15}.

Compared to traditional treatments, immunotherapy has been highlighted as an innovative cancer treatment that can lead to increased overall survival rates. With immunotherapy, the immune system can be strengthened by various agents, such as specific antibodies, cytokines, and checkpoint inhibitors, resulting in the activation of natural killer (NK) cells or T cells that destroy tumor cells^{16,17}. As cell-signaling molecules, cytokines help control the proliferation, differentiation, and function of immune cells and balance humoral and cell-mediated immune responses. Several cytokines, including interleukin (IL)-2, IL-12, IL-15, granulocyte macrophage colony stimulating factor (GM-CSF), and interferon (IFN)- γ , have been tested in clinical trials and animal cancer models. Sargramostim, a recombinant human GM-CSF (rhu GM-CSF), was approved by the FDA in 1991 to accelerate hematologic recovery in patients with non-Hodgkin's lymphoma, acute lymphocytic leukemia, or Hodgkin's disease^{18,19}. Anticancer effects were observed in patients treated with sargramostim, which might have depended on immune-modulating activity, such as dendritic cell (DC) activation, M1 polarization, and T cell infiltration into tumor tissues^{19–22}. However, the antitumor effect of sargramostim was not consistent in clinical trials or animal models of various types of cancer, including melanoma, and monotherapy did not show strong efficacy, probably due to contradicting activity depending on the concentration^{18,19}. Low GM-CSF concentrations can induce stimulation of antitumor responses, whereas high GM-CSF concentrations lead to tumor progression via regulatory T cell activation²³. In patients with extranodal NK/T cell lymphoma, accelerated tumor progression was also noted as a consequence of programmed death-ligand 1 (PD-L1)-mediated immune evasion induced by rhu GM-CSF monotherapy²⁴. As some cancer cells use PD-L1 to escape immune surveillance by interacting with programmed cell death-1 (PD-1) on immune cells, inhibiting PD-1-mediated signaling has been targeted for the development of cancer therapeutics^{25,26}. As immune-checkpoint inhibitors, PD-L1 inhibitors, such as atezolizumab, durvalumab, and avelumab, have been approved by the FDA to treat malignant tumors, including non-small cell lung cancer (NSCLC), triple-negative breast cancer, and Merkel cell carcinoma^{25,27}. The clinical outcome of PD-L1 inhibitor monotherapy has been shown to depend on high PD-L1 expression in cancer cells^{27,28}. However, combination therapy using PD-L1 inhibitors and chemotherapy can also improve patient outcomes after treatment for certain types of cancer, including NSCLC^{28,29}. In a murine model of metastatic melanoma, combined treatment with GM-CSF and a PD-1 inhibitor inhibited tumor growth and prolonged survival³⁰. Previous investigators have also proposed that such a combination

of cytokines and immune-checkpoint inhibitors can benefit patients with acquired resistance to immune-checkpoint inhibitors, including PD-L1 or CTLA4 inhibitors^{30–32}.

We developed a live, attenuated cancer vaccine using an engineered *Salmonella* strain that delivers recombinant GM-CSF through a flagellar T3SS in a controllable manner. First, a recombinant gene encoding GM-CSF with an N-terminal FlgM tag was expressed from a plasmid under the control of the P_{BAD} promoter. The attenuated *Salmonella* strain carrying the plasmid was tested for secretion of the recombinant protein, and immunostimulatory activity was also evaluated *in vitro*. The antitumor effect of the engineered *Salmonella* strain was monitored using a murine tumor model, which showed repressed tumor growth based on the activation of immune responses, such as M1 polarization and DC and CD8⁺ T cell recruitment into tumor tissues. Furthermore, tumor growth was drastically inhibited by administering the engineered *Salmonella* strain to tumor-bearing mice pretreated with a PD-L1 inhibitor, which resulted in survival gain. Finally, tumor growth was not observed in the tumor-bearing mice, even after tumor cell challenge, when they were pretreated with the PD-L1 inhibitor and subsequently with the engineered *Salmonella* strain. Certain protection against tumor recurrence was conferred by the stimulation of memory T cells, including both CD4⁺ and CD8⁺ cells. Our results show the strong potential of *Salmonella*-based cancer therapeutics as immunotherapy agents and cancer vaccines. Additionally, we demonstrated that the engineered *Salmonella* strain could support screening when evaluating cancer therapeutics by manipulating the genetic information of a candidate molecule or a combination of certain molecules.

2. Materials and methods

2.1. Bacterial strains and culture conditions

The ppGpp-defective strain SMR2130 ($\Delta relA \Delta spoT$) was derived from wild-type *Salmonella typhimurium* 14028s, as previously described³³, and was used as a host strain carrying a plasmid encoding GM-CSF with an N-terminal FlgM tag. All bacterial strains were grown overnight in LB broth at 37 °C. Ampicillin (100 µg/mL) and L-arabinose were added at the indicated concentrations when necessary. All compounds were purchased from Sigma–Aldrich (St. Louis, MO, USA).

2.2. Constructing a plasmid for GM-CSF secretion via the flagellar secretion system

A plasmid encoding recombinant GM-CSF was constructed by ligating a DNA fragment encoding GM-CSF with an N-terminal FlgM tag into pBAD33 after digestion with NheI (#R313; New England Biolabs, Ipswich, MA, USA) and HindIII (#R0104; New England Biolabs). The resulting plasmid was named pGMCSF. The *gm-csf* DNA fragment was synthesized by CosmoGenetech (Seoul, Korea), where codon-optimized *gm-csf* was located after *flgM*, and a 6 × His tag (with flanking GS linkers) was located between *flgM* and *gm-csf*. In addition, a synthetic ribosome-binding site (RBS) was introduced in front of *flgM* to increase expression of the recombinant gene. The coding sequences of *flhDC* together with the native RBS were further cloned into pGMCSF following ClaI digestion, blunt-end formation *via* Klenow fragment filling, and ligation, resulting in the pS-GMCSF

plasmid (Fig. 1A). pS-GMCSF was then transformed into the ppGpp[−] *Salmonella* strain SMR2130.

2.3. Measuring bacterial GM-CSF secretion using Western blot analysis

Overnight-grown SMR2130 bacteria carrying pS-GMCSF were freshly cultured in LB medium containing 0.04% (v/v) L-arabinose for 2 h at 37 °C, with vigorous aeration at 200 rpm, to induce FlgM-tagged GM-CSF expression. After the 2-h incubation period, the bacterial cells were harvested *via* centrifugation at 13,000 × *g* for 3 min. The resulting pellet was resuspended in 1 mL of 1 × phosphate-buffered saline (PBS), and the culture supernatant was passed through a filter unit with a 0.2 µm pore size. Each fraction was mixed with sodium dodecyl sulfate (SDS) loading buffer containing 0.2% β-mercaptoethanol. The whole-cell lysate was prepared using centrifugation without separation. The whole-cell lysate and each fraction were resolved *via* 12% SDS-polyacrylamide gel electrophoresis (PAGE), and the separated proteins were transferred to a nitrocellulose membrane (#LC7034-300; GenDEPOT, Katy, TX, USA) for Western blot analysis. The membranes were blocked in Tris-buffered saline with Tween (TBST) containing 5% skim milk powder (w/v). After the blocking step, the membranes were probed at room temperature (RT) for 1 h with an anti-His antibody (#sc-53073; Santa Cruz Biotechnology, Dallas, TX, USA) or an anti-GM-CSF antibody (#sc-398649; Santa Cruz Biotechnology) for GM-CSF or an anti-DnaK antibody (#PA5-117658; Thermo Fisher Scientific, Rochester NY, USA); each antibody was diluted 1:2000 (v/v) in TBST containing 2.5% skim milk powder (w/v). DnaK was used as a cytosolic protein marker. A horseradish peroxidase (HRP)-conjugated anti-mouse IgG antibody (#7076, for GM-CSF; Cell Signaling Technology, Danvers, MA, USA) or an anti-rabbit IgG antibody (#7074, for DnaK; Cell Signaling Technology) was used as a secondary antibody. Each secondary antibody was diluted 1:5000 in TBST containing 2.5% skim milk powder before incubating the membranes at RT for 1 h. The bands were detected on an iBright CL1500 Imaging system (Thermo Fisher Scientific) using a chemiluminescence substrate (#32209; Thermo Fisher Scientific).

2.4. Cell lines and bone marrow-derived macrophage (BMDM) cell preparation

The CT26 cell line (a murine colon carcinoma cell line from BALB/c mice) and the Raw264.7 cell line (a mouse macrophage-like cell line) were obtained from the American Type Culture Collection (Manassas, VA, USA). The CT26 cells were cultured in high-glucose Dulbecco's modified Eagle's medium (DMEM) supplemented with 10% fetal bovine serum (FBS; #S001-01; Welgene, Gyeongsan-si, Korea) and 1% penicillin-streptomycin (#LS202-02; Welgene) and maintained at 37 °C in 5% CO₂. The Raw264.7 cells were cultured in the same manner, except that RPMI 1640 was used instead of DMEM.

To isolate BMDMs, 8-week-old female C57BL/6 mice were euthanized, and bones were isolated from the legs after removing the skin, flesh, and muscles using sterile forceps and scissors. The bones were then crushed in 1 × PBS using a sterile mortar and pestle, and filtrates were collected *via* filtration through a cell strainer (#93040; SPL Life Sciences, Pocheon-si, Korea). Monocytes were cultured in RPMI 1640 + GlutaMAX medium (#61870036; Thermo Fisher Scientific) containing 10% FBS

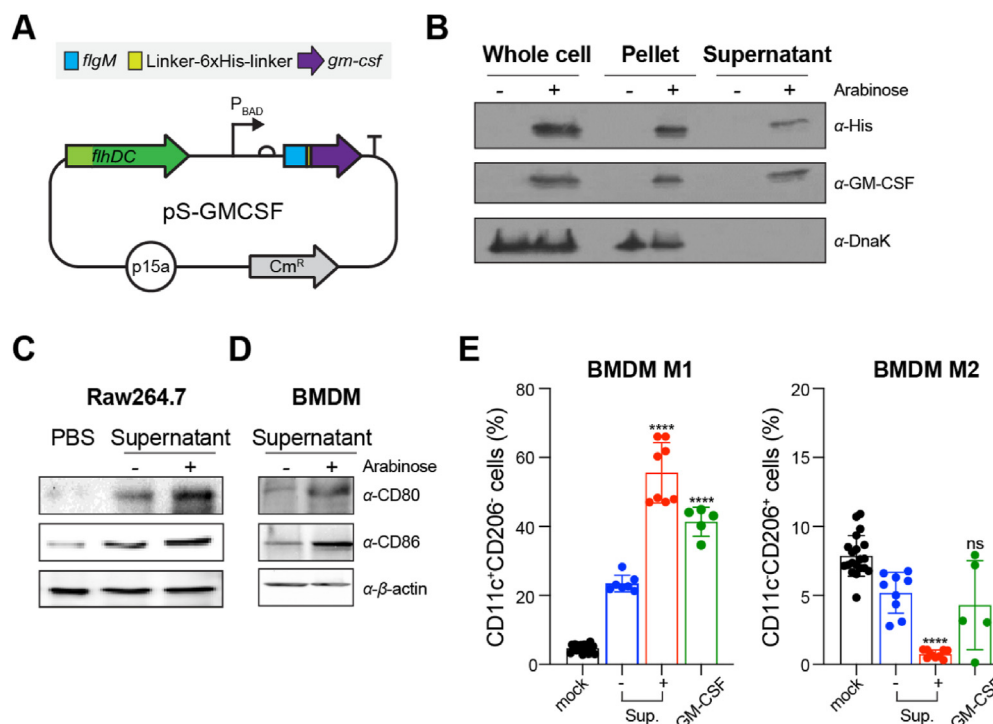


Figure 1 Macrophage polarization by FlgM-tagged GM-CSF secreted from *Salmonella*. (A) Map of pS-GMCSF for expression and secretion of recombinant GM-CSF, which is tagged with FlgM at the N-terminus and with GS linker together with 6 × His placed between FlgM and GM-CSF. (B) SMR2130 carrying pS-GMCSF was cultured in LB for 2 h at 37 °C, and the expression of FlgM-tagged GM-CSF was induced by the addition of 0.04% L-arabinose. After 2 h of further incubation at 37 °C, harvested cells were analyzed by Western blot using anti-His or anti-GM-CSF antibody. Anti-DnaK antibody was used as a cell lysis control. Experiments were repeated at least three times. Representative data are shown. (C–E) Raw264.7 cell lines (C) or BMDMs (D) were treated with PBS or bacterial culture supernatant containing 1 µg/mL total protein without (–) or with (+) induction by 0.04% L-arabinose. The expression of CD80 or CD86 was analyzed by Western blot. (C, D) β-Actin was used as a loading control. (E) BMDMs treated with culture supernatant with arabinose induction were analyzed via flow cytometry using antibodies. After gating with F4/80⁺ and CD11b⁺, cells were further sorted as CD11c⁺CD206⁺ for the M1 type or CD11c⁺CD206⁺ for the M2 type. Percent population was calculated by the number of each type of macrophage/total number of macrophages. Significance is shown as *****P* = 0.0001; ns = not significant. BMDM: bone marrow-derived macrophage; GM-CSF: granulocyte macrophage colony stimulating factor; PBS: phosphate-buffered saline.

(Welgene) and 1% penicillin-streptomycin cocktail after erythrocytes were removed from the supernatant using Red Blood Cell Lysing Buffer (ACK buffer, #10-548E; Lonza, Basel, Switzerland). Monocytes were then differentiated into M0 macrophages by adding culture supernatant from L929 cells (final concentration, 10%) to the media and culturing the cells for 7 days in a humidified CO₂ incubator at 37 °C³⁴.

2.5. Western blot analysis of CD80 and CD86 expression in Raw264.7 cells and BMDMs after treatment with secreted GM-CSF

For each assay, Raw264.7 or BMDM cells were seeded at a density of 5 × 10⁵ cells/mL and treated with 1 µg/mL of bacterial culture supernatant. The bacterial supernatant was prepared as described above for SMR2130 cells carrying pS-GMCSF, treated with or without arabinose. Each supernatant was concentrated using a centrifugal filter with a 3000 Da molecular weight cut-off (#UFC903008, 3K MWCO; Sigma–Aldrich). Recombinant GM-CSF (#130-095-746, 20 ng/mL; Miltenyi Biotec, Bergisch Gladbach, Germany) was used as a control. The treated cells were incubated for 24 h in a humidified CO₂ incubator at 37 °C and

lysed in radioimmunoprecipitation assay (RIPA) buffer (#R0278; Sigma–Aldrich) containing phosphatase and protease inhibitor cocktail (#78440; Thermo Scientific, Rochester NY, USA) and ethylenediaminetetraacetic acid (EDTA, 5 mmol/L, #78440; Thermo Scientific). The total protein concentrations in the cell lysates were quantified using the Bradford method, and each sample (containing 0.1 mg of total protein) was separated by 12% SDS-PAGE. Western blot analysis was performed using primary antibodies against CD80 (#sc-376012; Santa Cruz Biotechnology), CD86 (#sc-28347; Santa Cruz Biotechnology), or β-actin (#sc-47778; Santa Cruz Biotechnology). An HRP-conjugated anti-mouse IgG antibody was used as a secondary antibody.

2.6. Fluorescence activated cell sorting (FACS) analysis of polarized BMDMs

Using Enzyme Free Cell Dissociation Solution Hank's Based (#s-004; Sigma–Aldrich) and a scraper, BMDM cells were collected 24 h after treatment with 1 µg/mL of culture supernatant from SMR2130 cells carrying pS-GMCSF, which were treated with or without 0.04% L-arabinose or recombinant GM-CSF protein (20 ng/mL) as a control. The cells were then harvested via

centrifugation at $3500\times g$, and each pellet was resuspended in FACS buffer (Dulbecco's PBS containing 3% FBS, 0.1 mol/L EDTA, 50 U penicillin-streptomycin solution, and 1 mmol/L sodium pyruvate). Single-cell suspensions were stained with anti-F4/80-FITC (#11-4802-82; Invitrogen, Waltham, MA, USA), anti-CD11b-BV421 (#101236; BioLegend, San Diego, CA, USA), anti-CD11c-PE-Cy7 (#117318; BioLegend), and anti-CD206-APC (#141708; BioLegend) antibodies. Samples were analyzed on a FACSCanto II flow cytometer (BD Bioscience, San Jose, CA, USA) using FlowJo software (version 10.8).

2.7. Mouse tumor models

Female 6-week-old BALB/c and C57BL/6 mice were purchased from Orient Bio (Korea). All experiments and euthanasia were performed in accordance with protocols approved by the Chonnam National University Animal Research Committee (CNU IACUC-H-2022-14). Mice were implanted subcutaneously with 1×10^6 CT26 tumor cells into the right flank and injected intravenously (i.v.) with 1×10^7 colony-forming units (CFUs) of SMR2130 cells carrying pS-GMCSF when the tumors reached approximately $100\text{--}150\text{ mm}^3$. FlgM-tagged GM-CSF expression was induced by daily intraperitoneal administration of L-arabinose (100 mg/kg) at 3 days post-infection (dpi). To deplete PD-L1 in tumor-bearing mice, the mice were administered an anti-PD-L1 antibody (200 $\mu\text{g}/\text{mouse}$; #EB0101; BioXcell, Lebanon, NH, USA) through the intraperitoneal (i.p.) route at -3 , 0 , and 3 dpi. For the tumor-rechallenge model, CT26 tumor cells (1×10^6) were subcutaneously implanted into the left flank at 100 dpi. The mice were monitored for tumor volumes, body weights, and survival. Tumor volumes were calculated using the formula: $0.5 \times \text{length} \times \text{width} \times \text{height}$ of the tumor (in millimeters). When the tumor volume exceeded 1500 mm^3 , the mice were euthanized according to the ethical guidelines of the Animal Research Committee of CNU.

Mice were euthanized after anesthesia using a mixture of ketamine (200 mg/kg) and xylazine (10 mg/kg) at 3 dpi (6 h after L-arabinose injection). Tumor tissues were isolated to evaluate the delivery of FlgM-tagged GM-CSF using Western blotting or *via* immunofluorescence analysis of immune cells. After homogenizing the tumor tissues in RIPA buffer containing a phosphatase and protease inhibitor cocktail and 5 mmol/L EDTA, the lysates were centrifuged at $25,000\times g$ for 30 min at 4°C , and the resulting supernatants were filtered through a filter unit with a 0.2 μm pore size. The collected fractions were subjected to Western blotting using anti-His, anti-GM-CSF, and anti- β -actin antibodies.

2.8. Immunofluorescence analysis of tumor tissues

The isolated tumor tissues were fixed with 4% formaldehyde, embedded in optimal cutting temperature compound (OCT; SAKURA #4583, Japan), and stored at -80°C . The frozen samples were sliced into 7 μm -thick sections using a microtome-cryostat and mounted on (3-aminopropyl) triethoxysilane-coated slides. After washing with $1 \times \text{PBS}$ (pH 7.4) to completely remove the OCT, the slides were incubated with primary antibodies (diluted 1:100 in PBS) at 4°C overnight. We used primary antibodies against F4/80 (#abb6640; Abcam, Cambridge, UK), CD86 (#ab112490; Abcam), CD206 (#ab64693; Abcam), MHC class II (#ab139365; Abcam), CD11c (#97585; Cell Signaling

Technology), CD3 ϵ (#ab231775; Abcam), CD8 α (#ab22378; Abcam), and PD-L1 (#ab213480, 1:400; Abcam). The following day, the slides were washed with $1 \times \text{PBS}$ and incubated at RT for 2 h with an Alexa Fluor[®]488-conjugated goat anti-rat antibody (#A11006; Invitrogen), an Alexa Fluor[®]594-conjugated goat anti-rabbit antibody (#A11012; Invitrogen), or an Alexa Fluor[®]594-conjugated goat anti-mouse antibody (A11005; Invitrogen); these secondary antibodies were used at a 1:100 dilution. Nuclei were stained with ProLong Gold Anti-fade Reagent and DAPI (#P36935; Thermo Fisher Scientific). Images were captured using a confocal microscope (Zeiss Laboratories, Germany) and analyzed using ZEN 2.6 software. Representative images are shown, unless otherwise indicated.

2.9. Analysis of memory T cells in tumor-rechallenged mice using FACS

At 120 dpi, sterile forceps and scalpels were used to isolate spleens from mice originally treated with SMR2130 carrying pS-GMCSF and an anti-PD-L1 antibody, followed by CT26 rechallenge at 100 dpi. As a control, spleens were also isolated from untreated healthy mice. The organs were then crushed in RPMI 1640 containing 3% FBS, 50 U penicillin-streptomycin solution, and 10 mmol/L HEPES buffer, after which they were filtered through a cell strainer (#93070; SPL Life Sciences). Pellets were resuspended in RBC lysis buffer (Gibco ACK lysing buffer; #A1049201; Thermo Fisher Scientific) and centrifuged at $220\times g$ for 5 min. The resulting splenocytes were centrifuged at $220\times g$ for 5 min and then resuspended in RPMI 1640 containing 3% FBS, 50 U penicillin-streptomycin solution, and 10 mmol/L HEPES buffer. Splenocyte suspensions were stained with an APC-conjugated anti-mouse CD4 antibody (#100412; BioLegend), an FITC-conjugated anti-mouse CD8 α antibody (#100706; BioLegend), a PE/Cyanine7-conjugated anti-mouse CD62L antibody (#104418; BioLegend), CD44 Monoclonal Antibody eFluor[™] 450 (#48-0441-82; Invitrogen), or a PE-conjugated anti-mouse CD25 antibody. Subsequently, the splenocytes were analyzed using a FACSCanto II flow cytometer (BD Bioscience) with FlowJo software (version 10.8) to determine the types of memory T cells present in the samples.

2.10. Statistical analysis

All experimental data were analyzed using GraphPad Prism software (version 9.0). All data are presented as the mean \pm standard deviation (SD). Two-way analysis of variance with Tukey's correction was used to estimate differences between two groups, and the log-rank test (Mantel-Cox) was used to analyze the data from the survival experiments. Differences were considered statistically significant at $P < 0.05$.

3. Results

3.1. Effect of FlgM-tagged GM-CSF on macrophage M1 polarization

For targeted delivery into tumor tissues, we engineered an attenuated strain of *Salmonella* (ppGpp⁻; SMR2130) to express GM-CSF with an N-terminal FlgM tag. The FlgM-tagged GM-CSF variant was expressed from a pBAD33 plasmid (designated here

as the pGMCSF plasmid) under the control of an inducible P_{BAD} promoter and synthetic RBS (AGGAGGTTTGACCT). The FlgM target drives GM-CSF secretion into the extracellular space from the bacterial cytosol via the flagellar secretion system. In addition, the coding sequence of murine GM-CSF was optimized to increase its expression in *Salmonella*, and a $6 \times$ His tag (together with a GS linker) was encoded between FlgM and GM-CSF, which enabled detection and enhanced the flexibility of the recombinant protein. Furthermore, the master regulator of flagellum synthesis, FlhDC, was introduced into the plasmid to ensure that the protein was secreted from the ppGpp⁻ *Salmonella*, SMR2130 (Fig. 1A; pS-GMCSF plasmid). FlgM-tagged GM-CSF expression was specifically induced with 0.04% arabinose and clearly detectable in cell lysates and supernatant fractions from bacterial cultures with an anti-His or anti-GM-CSF antibody (Fig. 1B).

Next, we tested the function of secreted FlgM-tagged GM-CSF using cultured cell lines and primary cells. First, supernatants were prepared from *Salmonella* cultures 2 h after induction with 0 or 0.04% L-arabinose. Raw264.7 cells or BMDMs were each treated for 24 h with the supernatant fraction containing 1 μ g/mL of total protein, and macrophage surface markers were analyzed using Western blotting (Fig. 1C and D). M1 macrophage markers (CD80 and CD86) were expressed approximately 5-fold higher in Raw264.7 macrophages treated with supernatant containing FlgM-tagged GM-CSF than in those treated with PBS. Both markers were upregulated approximately 3-fold by the addition of the supernatant from non-induced, cultured Raw264.7 cells. Adding supernatant containing FlgM-tagged GM-CSF to BMDMs increased the expression levels of CD80 and CD86 4.7- and 2.7-fold, respectively, compared to the levels in cells treated with control supernatant lacking secreted GM-CSF. Notably, bacterial components (such as lipopolysaccharide) induce the expression of M1 macrophage markers, including CD80 and CD86³⁵. The percent population of BMDMs was characterized using flow cytometry, which revealed that M1 macrophages comprised 55.55% of the total macrophage population, based on gating CD11c⁺CD206⁻ samples from F4/80⁺CD11b⁺ cells treated with culture supernatant containing FlgM-tagged GM-CSF (Fig. 1E). The fraction of M1 macrophages also increased to 41.4% when BMDMs were treated with 1 μ g of recombinant GM-CSF. The fraction of M1 macrophages increased up to 23.43% when BMDMs were cultured with supernatant lacking secreted GM-CSF, which was consistent with our Western blot analysis of CD80 or CD86 expression levels. As expected, the fraction of M2 macrophages decreased following the addition of GM-CSF, either as purified protein (4.29%) or in the supernatant (0.58%), when compared to that in non-treated BMDMs (7.87%).

Taken together, our results indicate that FlgM-tagged GM-CSF was expressed and secreted from the engineered *Salmonella* strain and was functional as an immune-stimulating factor, including the capability to stimulate M1 macrophage polarization with expected anticancer effects.

3.2. Tumor-regressive effect of FlgM-tagged GM-CSF delivered by *Salmonella*

The antitumor effect of delivering FlgM-tagged GM-CSF with the *Salmonella* strain developed in this study was investigated using a mouse tumor model. CT26 tumor-bearing mice were i.v. challenged with the SMR2130 strain (carrying the pS-GMCSF plasmid), and L-arabinose was introduced by i.p. injection at 3 dpi to induce FlgM-tagged GM-CSF expression. FlgM-tagged

GM-CSF was detected in isolated tumor tissues 6 h after induction, indicating that the recombinant GM-CSF was delivered by the *Salmonella* SMR2130 strain carrying pS-GMCSF after expression by L-arabinose induction (Fig. 2A). Notably, the ppGpp-defective *Salmonella* strain accumulated at high levels in tumor tissues at 3 dpi^{34,36}.

The effects of FlgM-tagged GM-CSF on tumor regression were monitored by measuring tumor volumes, body weights, and mouse survival rates. Fig. 2B (images of tumors in all tested mice are shown in Supporting Information Fig. S1) shows representative images indicating that the tumor volumes were similar among all tested mice at 2 dpi but gradually decreased in mice injected with *Salmonella* carrying pS-GMCSF, and tumor growth slowed dramatically after L-arabinose administration. The tumor growth rate in mice treated with *Salmonella* that delivered FlgM-tagged GM-CSF evidently decreased over time (Fig. 2C). No changes in body weight were observed in any of the mice, indicating no signs of active infection (Fig. 2D). Further, the tumor-regressive effect of the delivered FlgM-tagged GM-CSF led to an increased lifespan of the tumor-bearing mice of up to 52 days (Fig. 2E). Therefore, our results suggest that the engineered *Salmonella* strain can serve as a delivery platform for cancer immunotherapy. However, GM-CSF delivery alone was not sufficient for complete remission in our mouse tumor model.

3.3. Stimulating immune cells in tumors with FlgM-tagged GM-CSF

Next, the immunostimulatory activity of FlgM-tagged GM-CSF was explored by profiling immune cells and molecular markers in tumor tissues. At 3 dpi, we excised tumor tissues from mice injected with PBS or SMR2130 carrying pS-GMCSF 6 h after L-arabinose (0 or 100 mg/kg) administration. The cells of all mice stained positively for F4/80 expression, indicating the presence of macrophages in their tumor tissues, and CD86-positive and CD206-negative cells were detected in the tumors of mice administered *Salmonella* carrying pS-GMCSF and arabinose (Fig. 3A and B). CD206-positive macrophages were identified in samples from mice treated with PBS or *Salmonella* carrying pS-GMCSF without arabinose administration. These results suggest that FlgM-tagged GM-CSF stimulates M1 macrophage polarization in tumors. Notably, macrophages recruited into the TME can control antitumor immune responses where M2 and M1 macrophages are involved in facilitating tumor growth and attacking tumor cells, respectively^{37,38}. M2 polarization induced by colony stimulating factor1 (CSF1) leads to tumor cell proliferation, and tumor growth is repressed by anti-CSF1 inhibitor or blocking of CSF1 receptor (CSF1R)^{39,40}. Indeed, we observed tumor regression in CT26-bearing mice by administration of anti-CSF1R suggesting the importance of macrophages in tumor immunotherapy (Supporting Information Fig. S2).

Other types of immune cells were also characterized based on surface markers. DCs (MHCII⁺ and CD11c⁺) or CD8⁺ T cells (CD3e⁺ and CD8 α ⁺) were distinctly detected in mouse tumors after arabinose induction and exposure to FlgM-tagged GM-CSF from tumor-targeted *Salmonella* (Fig. 3C and D). Our results showed that delivering FlgM-tagged GM-CSF increased DC or CD8⁺ T cell infiltration into tumors. Therefore, delivering GM-CSF using an engineered *Salmonella* strain can stimulate the immune system, resulting in improved tumor regression and an extended life span for tumor-bearing mice. However, tumor

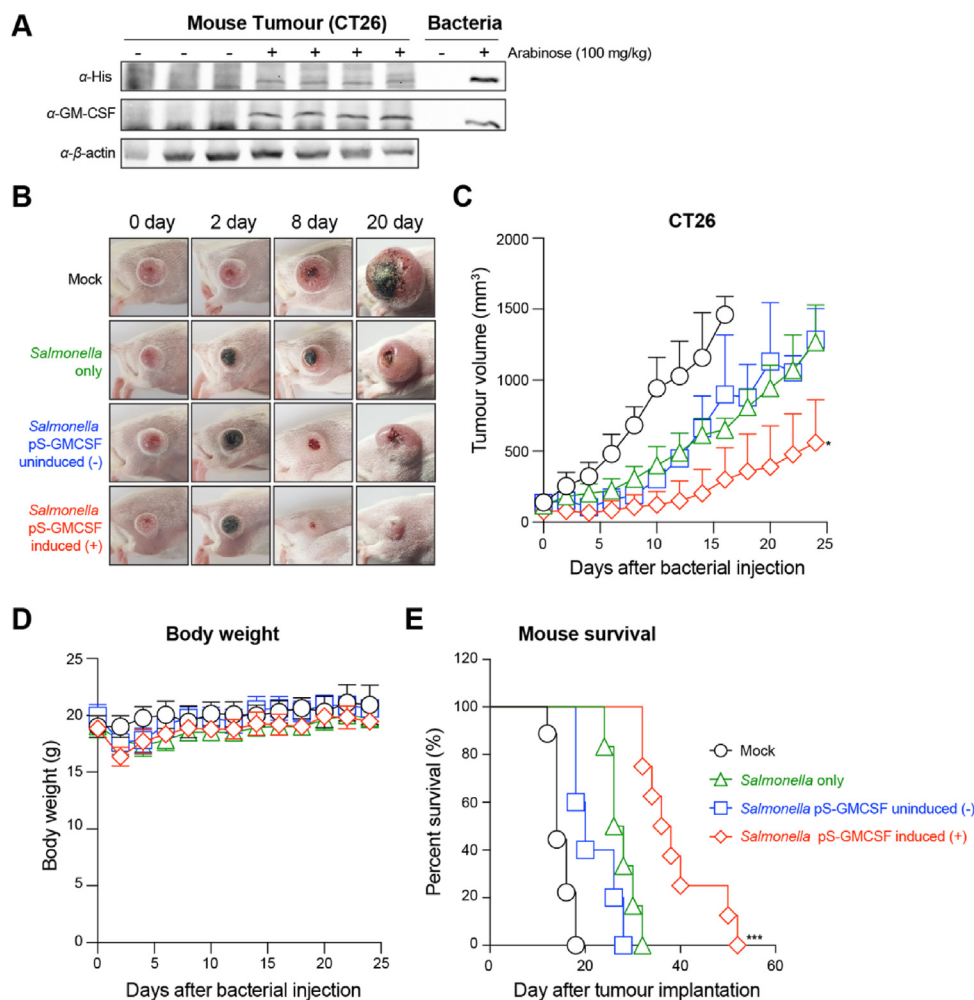


Figure 2 Tumor regression by FlgM tagged GM-CSF from tumor-targeted *Salmonella*. Tumor-bearing mice were administered 1 × PBS (mock) or SMR2130 (*Salmonella* only; green triangle) or SMR2130 carrying pS-GMCSF via the intravenous route. At 3 days post-infection, 1 × PBS (blue square; -) or arabinose (red diamond; 100 mg/kg; +) was introduced intraperitoneally into each group of mice. (A) FlgM-tagged GM-CSF from mouse tumor was detected by Western blot using anti-His or anti-GM-CSF antibody. The tumor was excised from mice 6 h after introduction of arabinose (+) or mock injection (-). Bacterial culture with or without the addition of arabinose (0.04%) was also used as a control for Western blot. β-Actin was used as a loading control. (B–E) Tumor growth was monitored daily. Representative images of tumors in mice are shown in B. Images of tumors in all tested mice are shown in [Supporting Information Fig. S1](#). The (C) tumor volume or (D) body weight was plotted as a function of time. Survival of each group of mice is presented in (E). Significance is shown as * $P = 0.0186$ and *** $P = 0.0003$. GM-CSF: granulocyte macrophage colony stimulating factor; PBS: phosphate-buffered saline.

growth was not fully repressed by FlgM-tagged GM-CSF. It has been reported that bacteria can stimulate PD-L1 overexpression in tumors, which may lead to cancer progression. GM-CSF itself can induce immune evasion by increasing PD-L1 expression in certain types of tumors, including lymphomas^{24,41}. Collectively, our findings suggest that FlgM-tagged GM-CSF from the engineered *Salmonella* strain could induce antitumor immune responses (including M1 macrophage polarization and DC and CD8⁺ T cell recruitment into tumor tissues) but could also promote tumor progression by upregulating PD-L1 expression.

3.4. Tumor diminution by the engineered *Salmonella* strain and PD-L1 depletion

As FlgM-tagged GM-CSF could mediate adverse effects by increasing PD-L1 expression, CT26 tumor-bearing mice were challenged with a PD-L1-specific antibody 3 days before,

immediately before, or 3 days after administering the engineered *Salmonella* strain (Fig. 4A). PD-L1 depletion did not affect tumor growth when applied alone, but the visible tumor mass completely disappeared after combination treatment with PD-L1 depletion and FlgM-tagged GM-CSF delivery by the engineered *Salmonella* strain (Fig. 4B and C. Images of all tested mice are also shown in [Supporting Information Fig. S3](#)). The body weights of the tested mice did not change after any treatment, indicating that no infection-related responses occurred (Fig. 4D). Finally, combination treatment improved the survival rate of the tumor-bearing mice by 25% (Fig. 4E). The synergistic effect of the combination treatment was not limited to a single mouse tumor model. The effect was also observed in mice implanted with other cancer cell lines, such as the MC38 cell line, which showed an even better improvement in the survival rate than mice with CT26 cell-derived tumors ([Supporting Information Fig. S4](#)). These results suggest that the anticancer effect of FlgM-tagged GM-CSF can be boosted

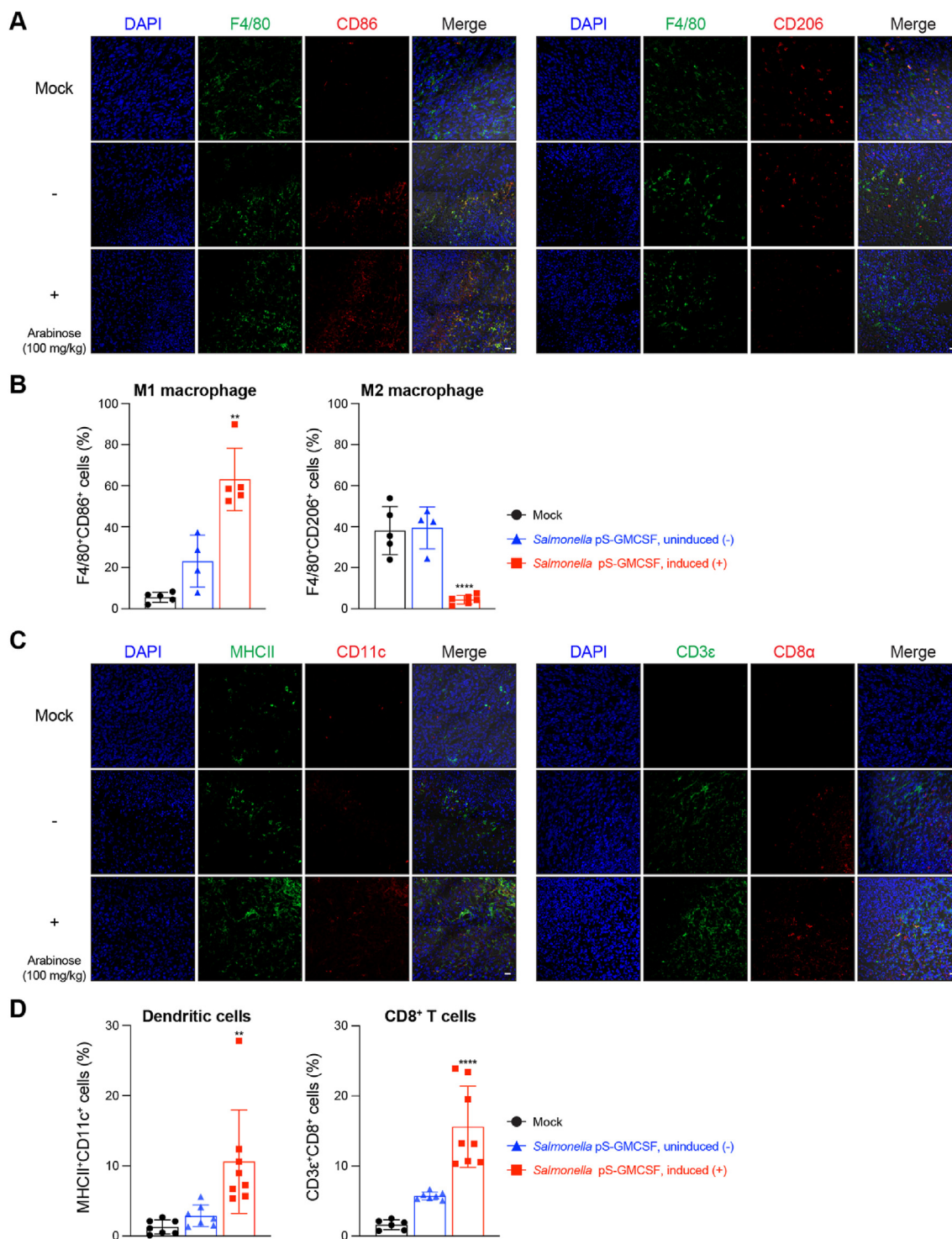


Figure 3 Effect of *Salmonella*-delivered FlgM-tagged GM-CSF on profiles of immune cells in tumor tissue. Tumor-bearing mice were administered $1 \times$ PBS (mock) or SMR2130 carrying pS-GMCSF through the tail vein, and $1 \times$ PBS (–) or arabinose (+) was injected at 3 days post-infection through the intraperitoneal route. After 6 h, tumor tissues were excised, fixed, and processed for immunofluorescence analysis. (A) Macrophages were detected with anti-F4/80 antibody and further analyzed using anti-CD86 antibody for the M1 type or anti-CD206 antibody for the M2 type. Percent population of each type of macrophage is presented in (B). (C) Dendritic cells were identified with anti-MHCII and anti-CD11c antibodies, and CD8⁺ T cells with anti-CD3ε and anti-CD8α antibodies. Nuclei of cells were detected with DAPI staining. Percent fractions of DCs or CD8⁺ T cells in tumor tissues are shown in (D). Scale bar indicates 20 μm. GM-CSF: granulocyte macrophage colony stimulating factor; PBS: phosphate-buffered saline; DAPI: 4',6-diamidino-2-phenylindole. Significance is shown as ** $P < 0.005$ and **** $P \leq 0.0001$.

by targeted delivery *via* tumor-targeting *Salmonella* and down-regulating immune checkpoint markers, such as PD-L1.

3.5. Engineered *Salmonella*-based cancer vaccine adjuvant

Next, we further studied the potential of the engineered *Salmonella* strain in cancer therapy by assessing its preventive activity against cancer recurrence. The protective effect was monitored by measuring the tumor volume and characterizing the types of T cells in tumors. To this end, tumor-bearing mice were injected with an anti-PD-L1 antibody for PD-L1 depletion

on Days -3, 0, and 3. The engineered *Salmonella* delivering FlgM-tagged GM-CSF was introduced i.v. on Day 0, and arabinose was administered at 3 dpi, since this combination showed the most dramatic tumor volume reduction and survival gain. On Day 100, CT26 cells were subcutaneously implanted at a site opposite the first implantation site (Fig. 5A). Fig. 5B shows a representative *in vivo* image indicating that the second tumor disappeared before 150 dpi. Tumor volumes were monitored in 13 mice that were rechallenged with CT26 tumor cells, and tumor growth was not detected in any of these mice (Fig. 5C).

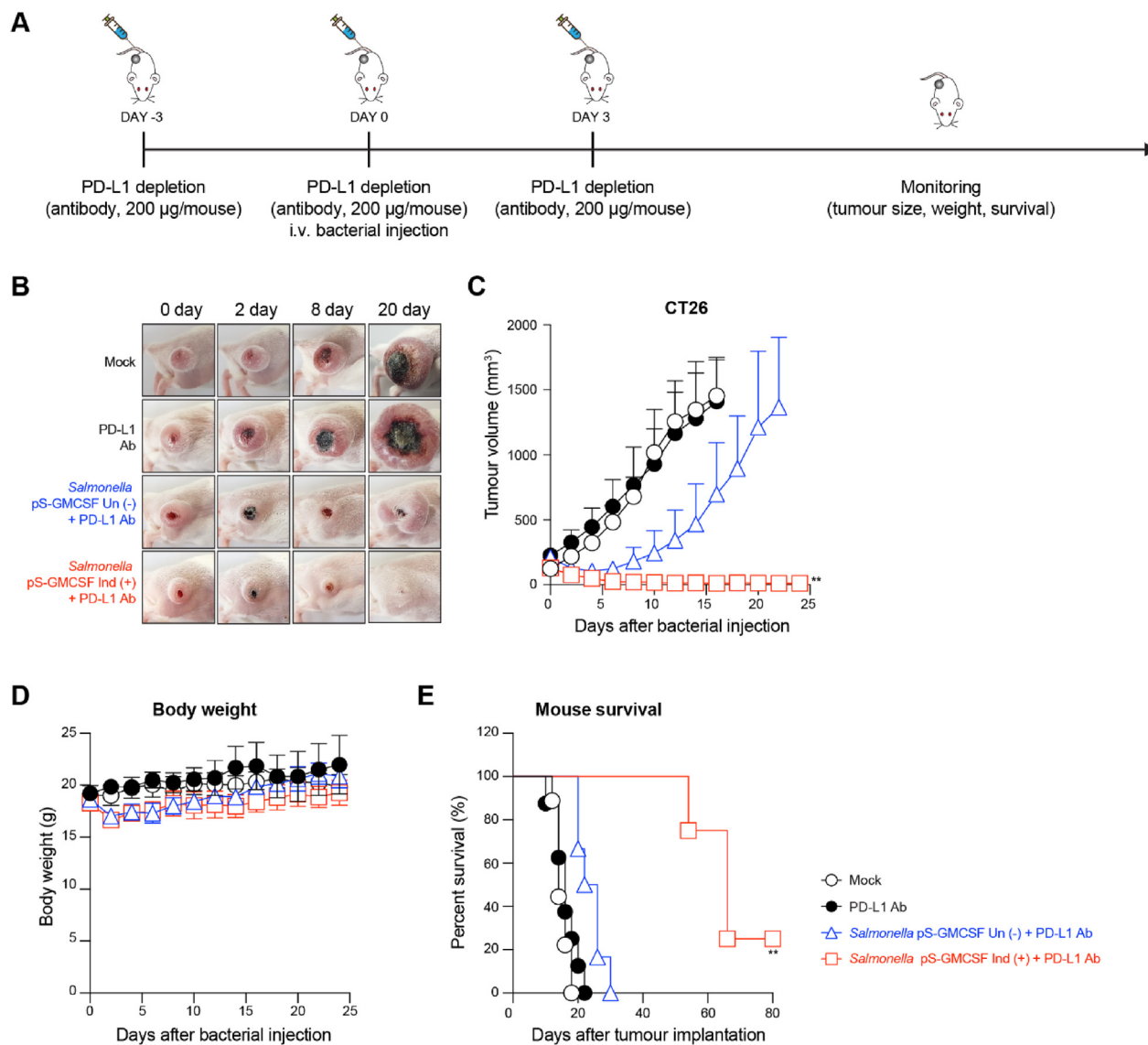


Figure 4 Combination effect of *Salmonella*-delivered FlgM-tagged GM-CSF and anti-PD-L1 antibody on tumor growth. (A) Experimental timeline is shown. PD-L1 depletion was achieved by intraperitoneal injection of anti-PD-L1 antibody (200 µg/mouse) at -3, 0, and 3 days post-infection. SMR2130 carrying pS-GMCSF was administered by i.v. injection on Day 0 (1×10^7 CFU), and L-arabinose (100 mg/kg) was introduced intraperitoneally. The group of tumor-bearing mice was injected with 1 × PBS (mock; $n = 8$) or anti-PD-L1 antibody as scheduled (PD-L1 Ab; black line and symbol; $n = 7$) as controls. L-Arabinose was introduced into one group of mice treated with *Salmonella* carrying pS-GMCSF (red line and symbol (+); $n = 8$), and 1 × PBS was injected into another group (blue line and symbol (-); $n = 6$) together with PD-L1 depletion. (B) Representative images are shown, and the measured (C) tumor volume, (D) body weight, and (E) survival of tumor-bearing mice under each treatment are shown by date. Images of all tested mice are also shown in Fig. S3. Significance is indicated as $**P = 0.005$. CFU: colony-forming unit; GM-CSF: granulocyte macrophage colony stimulating factor; i.v.: intravenous; PBS: phosphate-buffered saline; PD-L1: programmed death-ligand 1.

GM-CSF is an immune-modulating cytokine involved in macrophage maturation and functioning under normal health conditions, as well as cytotoxic T cell priming in patients with cancer⁴². Therefore, we sorted different types of memory T cells in samples from treated mice to elucidate the tumor-suppressive mechanism elicited by delivering the engineered *Salmonella* strain and depleting PD-L1. Compared to cells from non-treated healthy mice, the percentages of CD44⁺CD62L⁺CD4⁺ and CD44⁺CD62L⁺CD4⁺ T cells increased 1.6–2-fold, indicating that combined treatment with the engineered *Salmonella* strain and the anti-PD-L1 antibody expanded the populations of both effector and central memory CD4⁺ T cells (Fig. 5D). Likewise, the percentages of effector and central memory CD8⁺ T cells were increased 2.8–3.4-fold in mice administered the same treatment (Fig. 5E). In addition, the number of AH1⁺CD8⁺ T cells increased 6.3-fold following combination treatment, suggesting that the failure of new tumor growth resulted from the role of AH1 as a tumor-rejection antigen (Supporting Information Fig. S5)⁴³. Collectively, our findings indicate that the engineered *Salmonella* strain (delivering FlgM-tagged GM-CSF) can serve as a strong cancer vaccine adjuvant in combination with depletion of PD-L1.

4. Discussion

Clinical trials involving the use of bacteria for cancer treatment are ongoing, where a biological agent(s) with anticancer potency can be specifically delivered into a TME by bacteria with tumor-targeting ability⁴⁴. Furthermore, recent progress in genetic-manipulation techniques has made bacterial cancer therapy more accurate and controllable, which has reduced the chance of off-target delivery of an anticancer agent(s). Intrinsic factors of pathogens, such as flagella, can offer additional benefits by boosting immune responses⁷. Previous data have shown that cell-destroying factors are efficiently discharged by targeted bacteria and can substantially decrease tumor volumes in mice. However, incomplete elimination of tumor cells led to subsequent regrowth of solid tumors^{45–47}. Therefore, longer-lasting control of tumors is required to repress recurrence, which can be achieved by strengthening the immune system to recognize and destroy tumor cells.

In this study, we designed and engineered a *Salmonella* strain expressing GM-CSF under the control of an exogenous inducer, which could be delivered into tumors through the flagellar secretion system. ppGpp-defective *Salmonella* was used as a host for bacteria-based cancer immunotherapy because this bacterium can target tumor tissues with impaired infectivity in mice^{7,33,45,48}. Although heterologous cargo molecules, such as therapeutic proteins, can be expressed by bacteria in a user-controlled manner, the ability to deliver the expressed proteins to specific tissues is highly limited. However, a previous study showed that delivery could be carried out when host bacteria were lysed after reaching the intended target, resulting in the transient eradication of tumor cells⁴⁹. Fusion with signal peptides (such as PelB) was also used to promote protein translocation to the periplasm through general secretory pathways, such as the SEC pathway, and then to the extracellular space⁴⁵. However, such fusion was not always successful, resulting in a low chance of secretion into the target site, probably due to destabilization or aggregation of the fusion protein⁵⁰.

Therefore, we harnessed a bacterial secretion system for more controllable delivery of therapeutic proteins, where the cargo was

directly translocated from the bacterial cytosol to the extracellular space, that is, the TME, without a two-step transit process *via* the periplasm. During flagellar assembly, FlgM is secreted extracellularly, acts as a master regulator of flagellum synthesis, and can support the secretion of recombinant proteins when fused to the N-terminus of a protein of interest in bacteria^{15,51}. Consequently, recombinant GM-CSF was secreted into the bacterial culture medium *in vitro* and in tumor tissues *via* tumor-targeting *Salmonella* by introducing FlgM at the N-terminus of GM-CSF and overexpressing FlhDCs. Despite FlgM tagging, the secreted form of GM-CSF fully promoted the M1 polarization of M0 macrophages *in vitro*. FlgM-tagged GM-CSF was delivered into the tumor, which resulted in tumor regression and increased lifespan of CT26-tumour bearing mice. Immune cells were detected in tumor tissue stimulated by the delivered FlgM-tagged GM-CSF, including M1-type macrophages, DCs, and CD8⁺ T cells in a mouse model. Nevertheless, FlgM-tagged GM-CSF could not thoroughly eradicate tumors or extend the survival times of tumor-bearing mice.

The interaction between PD-1 and PD-L1 can promote immune tolerance within tumors by inhibiting T cell activation, proliferation, cytokine release, and survival⁵². Many tumor cells overexpress PD-L1 on their surface, thereby leading to suppressed T cell responses against cancer⁵³. Upregulated PD-L1 expression was also identified in our mouse tumor model. Therefore, the imperfect control of tumor growth may be attributable to immune tolerance induced by PD-L1 overexpression, despite immune stimulation by the delivered FlgM-tagged GM-CSF protein. The effect of PD-L1 depletion was validated in tumor-bearing mice treated with *Salmonella* that delivered FlgM-tagged GM-CSF. Mice treated with the PD-L1 antibody and *Salmonella*-delivered FlgM-tagged GM-CSF showed increased survival (up to 25%) and lower tumor volumes than mice only treated with the PD-L1 antibody or the engineered *Salmonella* strain. A complete cure can only be achieved by tightly controlling the delivery of an optimal dosage of GM-CSF, since GM-CSF itself can also induce tumor progression by regulating various pro-tumorigenic immune responses, such as the upregulation of immune check point molecules²³. Thus, optimal timing intervals and dosages for combination therapy should be investigated in future studies to attain a “cancer-free” state. Although some mice still carried tumors after treatment with engineered *Salmonella* and the PD-L1 antibody (13 of 25 mice), protection against newly developed tumors was evident. Such a vaccination effect relied upon the increased proportions of both CD4⁺ and CD8⁺ memory T cells, indicating that a synergistic effect was achieved by combination treatment with *Salmonella*-based cancer therapy that triggered an immune response (*via* cytokine and checkpoint inhibitor delivery) that stimulated T cell activation and differentiation.

Our study provides proof-of-concept for incorporating bacterial cancer therapy into conventional immunotherapy to improve the treatment efficacy. Cytokines, including GM-CSF, have been used for cancer therapy based on their tumor-suppressive effects; however, cytokines can also elicit tumor-promoting effects, such as polarizing macrophages to the M2 phenotype and upregulating immune checkpoint proteins. To overcome unfavorable consequences and maximize anti-tumor effects, cytokine-based cancer therapy can be revamped by optimizing the dosage and combination with other therapies. For this, engineered bacteria are excellent candidates to fulfil the conditions for cytokine-based therapy. Intrinsic factors, such as flagellin and lipopolysaccharide, can serve as immune boosters, and the desired cytokine can be

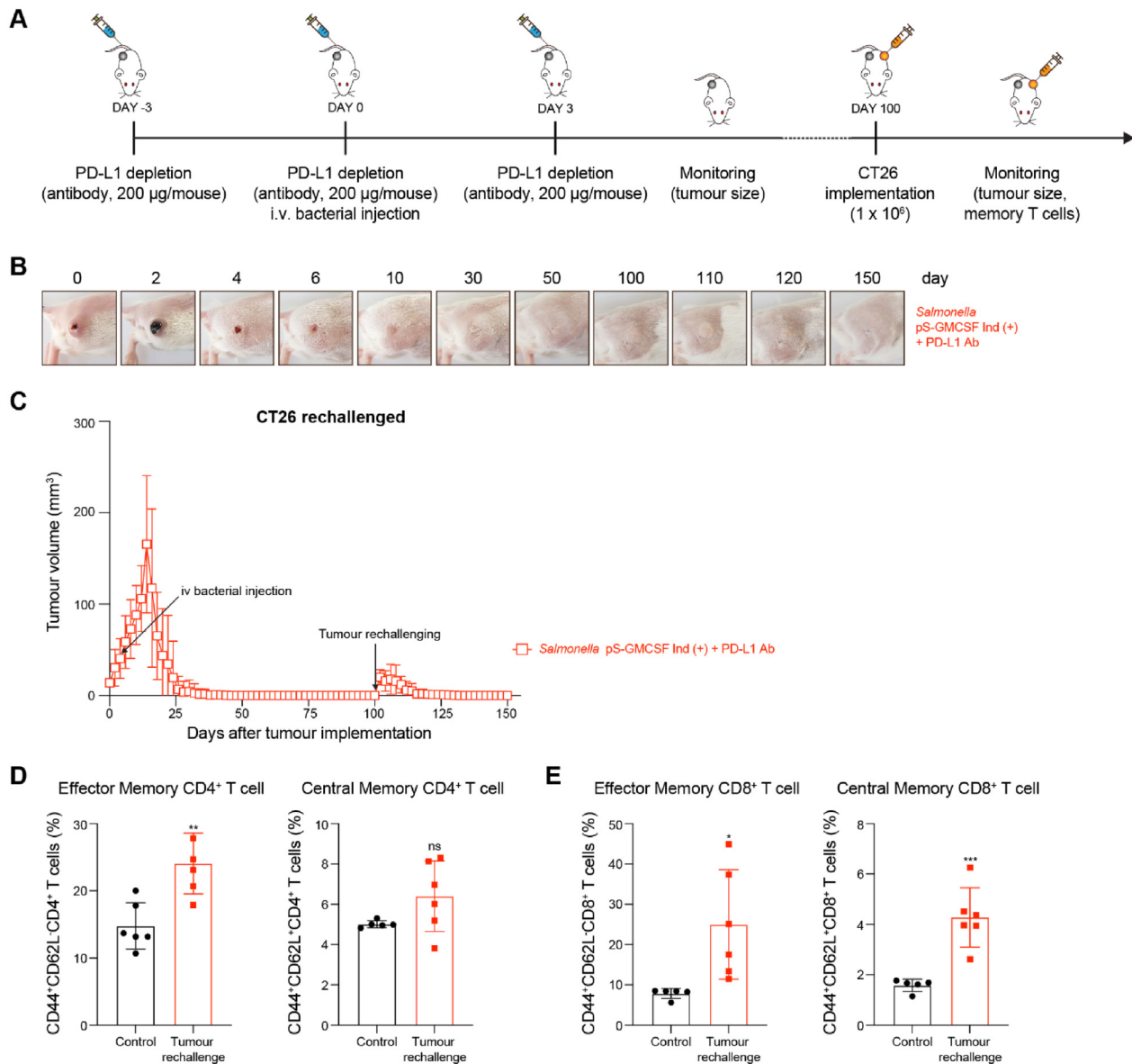


Figure 5 Stimulation of immune memory for the tumor by *Salmonella*-delivered FlgM-tagged GM-CSF and PD-L1 depletion. (A) Schematic of CT26 tumor rechallenge experiment. Mice bearing CT26 on the right flank were subjected to PD-L1 depletion using anti-PD-L1 antibody (200 µg/mouse) *via* intraperitoneal injection at -3, 0, and 3 dpi. On Day 0, SMR2130 carrying pS-GMCSF was administered to mice through the tail vein (1 × 10⁷ CFU). Tumor volume was monitored daily, and CT26 cells (1 × 10⁶) were subcutaneously implanted into the left flank (the opposite site to the first implantation position) at 100 dpi. (B) Representative images of mice treated with PD-L1 antibody and FlgM-tagged GM-CSF delivered by *Salmonella*, followed by CT26 rechallenge at 100 dpi. (C) Tumor volume was measured daily after tumor implantation. (D, E) Splenocytes were isolated from the tumor-rechallenged mice at 120 dpi. As a control, spleen cells were prepared from healthy mice. The isolated splenocytes were analyzed to identify T cell types using a FACSCanto II flow cytometry and FlowJo software. First, cells were identified as CD4⁺ or CD8⁺ T cells, and effector or memory cells were further sorted based on the detection of CD44⁺CD62L⁻ or CD44⁺CD62L⁺, respectively. Significance is shown as **P* = 0.0214, ***P* = 0.0063, and ****P* = 0.0007; ns = not significant. dpi: days post-infection; GM-CSF: granulocyte macrophage colony stimulating factor; PD-L1: programmed death-ligand 1.

genetically encoded for controllable expression and effective spatiotemporal delivery. In addition, bacterial cancer therapy can be combined with other therapeutic agents, as shown in this study by using GM-CSF-secreting *Salmonella* together with checkpoint inhibitors. We demonstrated antitumor responses using the combined treatment strategy, such as increased levels of M1 macrophages, DCs, and T cells, leading to tumor regression and protection against tumor recurrence with no systemic toxicity

(Fig. 6 and Supporting Information Fig. S6). Notably, neutralizing antibody against GM-CSF secreted by *Salmonella* was not detected in CT26-bearing mice at 18 dpi, which indicated that there were no specific immune responses against the FlgM-tagged GM-CSF delivered by the engineered *Salmonella* (Supporting Information Fig. S7).

Bacterial cancer therapy has strong potential because multiple anticancer agents can be expressed, and tight delivery control is

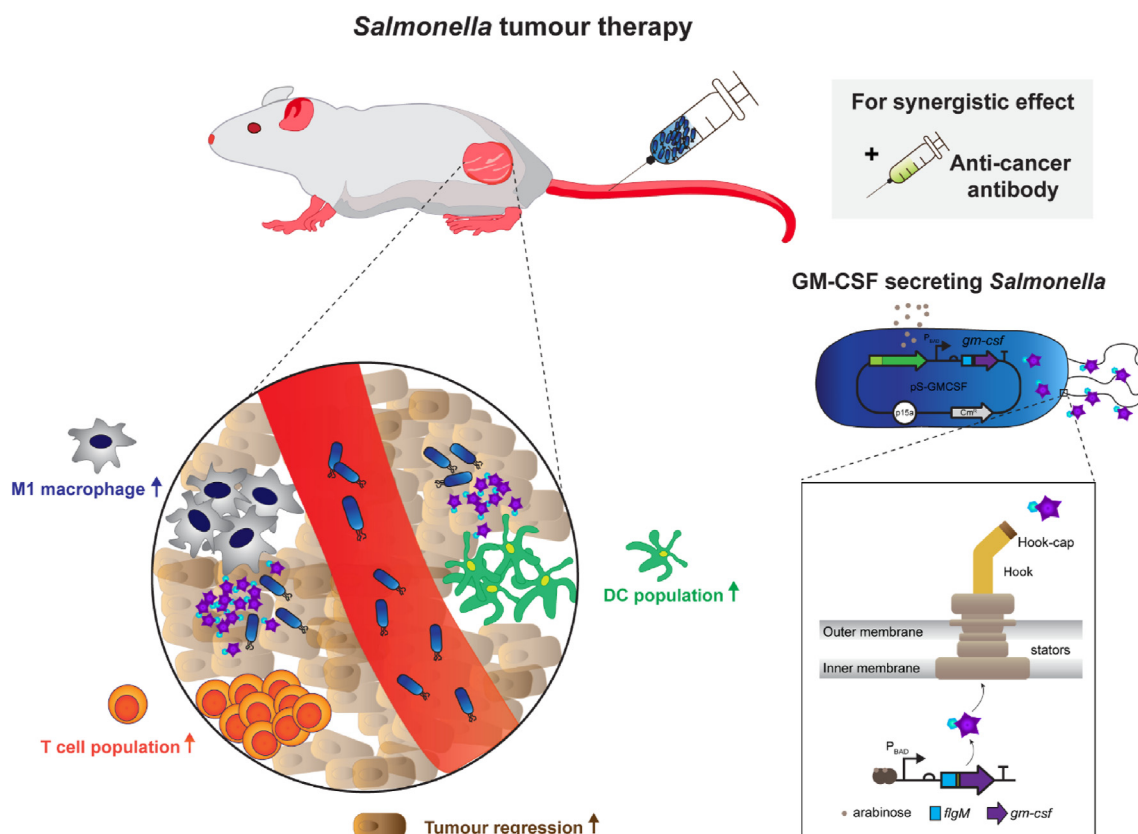


Figure 6 Model illustration for the engineered *Salmonella*-based cancer immunotherapy and vaccination. The attenuated *Salmonella* specifically targets tumor tissue and then secretes the recombinant GM-CSF via the flagella type 3 secretion system by the FlgM secretion tag, causing immune cells to be recruited into the tumor tissue, including M1 macrophages, DCs, and T cells, and ultimately resulting in increased tumor regression. Introduction of anticancer antibodies, such as PD-L1 inhibitors, maximizes immune responses against tumors via a synergistic effect. DC: dendritic cell; GM-CSF: granulocyte macrophage colony stimulating factor; PD-L1: programmed death-ligand 1.

feasible by engineered secretion systems. Bacteria have various secretion systems dedicated to the translocation of DNA or protein molecules from the bacterial cytosol to the extracellular space or even directly into the cytosol of mammalian cells^{54,55}. Several findings have shown that heterologous proteins can be delivered through an engineered T3SS *in vitro* or *in vivo*, as in this study^{56–58}. However, secretion control still relies upon exogenous inducers. Therefore, a controller system should be developed, such as a biosensor that can induce the expression of engineered cargo and delivery systems after sensing subtle changes in the TME. In addition, other cargo molecules, such as checkpoint inhibitors (*e.g.*, PD-L1) might be engineered in bacteria together with cytokines, thereby maximizing the antitumor activity of the engineered bacteria. Finally, engineered bacteria can serve as a superb testbed for discovering the best combinations of anticancer agents that can be used for other types of treatment, including cancer immunotherapy.

5. Conclusions

We described a live, attenuated cancer therapeutic agent that uses an engineered *Salmonella* strain that secretes GM-CSF through a flagellar system in a controllable manner. This research shows the strong potential of *Salmonella*-based cancer therapeutics as immunotherapy agents and cancer vaccine adjuvants.

Additionally, it demonstrates that the engineered *Salmonella* strain can support screening when evaluating cancer therapeutics by manipulating the genetic information of a candidate molecule or a combination of certain molecules.

Acknowledgments

This work was supported by National Research Foundation of Korea grants funded by the Korean government (NRF-2022R1A2C1009875, NRF-2017R1A5A2015385, and NRF-2018M3A9H3023081, Korea) and by the Korea Health Technology R&D Project through the Korea Health Industry Development Institute (KHIDI), funded by the Ministry of Health and Welfare, Republic of Korea (HR20C0025). Heung Jin Jeon was supported by NRF-2020R1A6A3A01099531 (Korea). Daejin Lim was supported by NRF-RS-2023-00210053 (Korea). Jae-Ho Jeong was supported by NRF-2020R1A5A2031185 (Korea). Miryoung Song was supported by NRF-2022M3E5F1018375, 2019M3E5D5066666 and the Hankuk University of Foreign Studies Research Fund of 2024 (Korea).

Author contributions

Heung Jin Jeon: Conceptualization, Formal analysis, Investigation. Daejin Lim: Conceptualization, Formal analysis, Investigation, Writing – original draft, Writing – review & editing. EunA.

So: Investigation. Solbi Kim: Investigation. Jae-Ho Jeong: Conceptualization, Writing – original draft, Writing – review & editing. Miryoung Song: Data curation, Formal analysis, Writing – original draft, Writing – review & editing. Hyo-Jin Lee: Conceptualization, Funding acquisition, Writing – original draft, Writing – review & editing.

Conflicts of interest

The authors have no competing interests to declare.

Appendix A. Supporting information

Supporting data to this article can be found online at <https://doi.org/10.1016/j.apsb.2024.07.011>.

References

- Patyar S, Joshi R, Byrav DSP, Prakash A, Medhi B, Das BK. Bacteria in cancer therapy: a novel experimental strategy. *J Biomed Sci* 2010; **17**:21.
- Guallar-Garrido S, Julián E. Bacillus Calmette-Guérin (BCG) therapy for bladder cancer: an Update. *Immunotargets Ther* 2020; **9**:1–11.
- Kasinskas RW, Forbes NS. *Salmonella typhimurium* specifically chemotax and proliferate in heterogeneous tumor tissue *in vitro*. *Bio-technol Bioeng* 2006; **94**:710–21.
- Liang K, Liu Q, Li P, Han Y, Bian X, Tang Y, et al. Endostatin gene therapy delivered by attenuated *Salmonella typhimurium* in murine tumor models. *Cancer Gene Ther* 2018; **25**:167–83.
- Din MO, Danino T, Prindle A, Skalak M, Selimkhanov J, Allen K, et al. Synchronized cycles of bacterial lysis for *in vivo* delivery. *Nature* 2016; **536**:81–5.
- Zhao T, Wei T, Guo J, Wang Y, Shi X, Guo S, et al. PD-1-siRNA delivered by attenuated *Salmonella* enhances the antimelanoma effect of pimezone. *Cell Death Dis* 2019; **10**:164.
- Zheng JH, Nguyen VH, Jiang SN, Park SH, Tan W, Hong SH, et al. Two-step enhanced cancer immunotherapy with engineered *Salmonella typhimurium* secreting heterologous flagellin. *Sci Transl Med* 2017; **9**:eaak9537.
- Das C, Mokashi C, Mande SS, Saini S. Dynamics and control of flagella assembly in *Salmonella typhimurium*. *Front Cell Infect Microbiol* 2018; **8**:36.
- Haiko J, Westerlund-Wikström B. The role of the bacterial flagellum in adhesion and virulence. *Biology* 2013; **2**:1242–67.
- Rossez Y, Wolfson EB, Holmes A, Gally DL, Holden NJ. Bacterial flagella: twist and stick, or dodge across the kingdoms. *PLoS Pathog* 2015; **11**:e1004483.
- Minamino T, Kinoshita M, Namba K. Insight into distinct functional roles of the flagellar ATPase complex for flagellar assembly in *Salmonella*. *Front Microbiol* 2022; **13**:864178.
- Mousslim C, Hughes KT. The effect of cell growth phase on the regulatory cross-talk between flagellar and *Spi1* virulence gene expression. *Plos Pathog* 2014; **10**:e1003987.
- Chadsey MS, Hughes KT. A multipartite interaction between *Salmonella* transcription factor sigma28 and its anti-sigma factor FlgM: implications for sigma28 holoenzyme destabilization through stepwise binding. *J Mol Biol* 2001; **306**:915–29.
- Gupta S, Bram EE, Weiss R. Genetically programmable pathogen sense and destroy. *ACS Synth Biol* 2013; **2**:715–23.
- Heel T, Vogel GF, Lammirato A, Schneider R, Auer B. FlgM as a secretion moiety for the development of an inducible type III secretion system. *PLoS One* 2013; **8**:e59034.
- Tan S, Li D, Zhu X. Cancer immunotherapy: pros, cons and beyond. *Biomed Pharmacother* 2020; **124**:109821.
- Waldman AD, Fritz JM, Lenardo MJ. A guide to cancer immunotherapy: from T cell basic science to clinical practice. *Nat Rev Immunol* 2020; **20**:651–68.
- Waldmann TA. Cytokines in cancer immunotherapy. *Cold Spring Harb Perspect Biol* 2018; **10**:a028472.
- Lazarus HM, Ragsdale CE, Gale RP, Lyman GH. Sargramostim (rhu GM-CSF) as cancer therapy (systematic review) and an immunomodulator. A drug before its time?. *Front Immunol* 2021; **12**:706186.
- Hong IS. Stimulatory versus suppressive effects of GM-CSF on tumor progression in multiple cancer types. *Exp Mol Med* 2016; **48**:e242.
- Boutillier AJ, ElSawa SF. Macrophage polarization states in the tumor microenvironment. *Int J Mol Sci* 2021; **22**:6995.
- Wei XX, Chan S, Kwek S, Lewis J, Dao V, Zhang L, et al. Systemic GM-CSF recruits effector T cells into the tumor microenvironment in localized prostate cancer. *Cancer Immunol Res* 2016; **4**:948–58.
- Kumar A, Taghi Khani A, Sanchez Ortiz A, Swaminathan S. GM-CSF: a double-edged sword in cancer immunotherapy. *Front Immunol* 2022; **13**:901277.
- Rong QX, Wang F, Guo ZX, Hu Y, An SN, Luo M, et al. GM-CSF mediates immune evasion via upregulation of PD-L1 expression in extranodal natural killer/T cell lymphoma. *Mol Cancer* 2021; **20**:80.
- Bagchi S, Yuan R, Engleman EG. Immune checkpoint inhibitors for the treatment of cancer: clinical impact and mechanisms of response and resistance. *Annu Rev Pathol* 2021; **16**:223–49.
- Yi M, Niu M, Xu L, Luo S, Wu K. Regulation of PD-L1 expression in the tumor microenvironment. *J Hematol Oncol* 2021; **14**:10.
- Morad G, Helmink BA, Sharma P, Wargo JA. Hallmarks of response, resistance, and toxicity to immune checkpoint blockade. *Cell* 2021; **184**:5309–37.
- Di Federico A, De Giglio A, Parisi C, Gelsomino F, Ardizzone A. PD-1/PD-L1 inhibitor monotherapy or in combination with chemotherapy as upfront treatment for advanced NSCLC with PD-L1 expression $\geq 50\%$: selecting the best strategy. *Crit Rev Oncol Hematol* 2021; **160**:103302.
- Jung HA, Park S, Choi YL, Lee SH, Ahn JS, Ahn M-J, et al. Continuation of pembrolizumab with additional chemotherapy after progression with PD-1/PD-L1 inhibitor monotherapy in patients with advanced NSCLC: a randomized, placebo-controlled phase II study. *Clin Cancer Res* 2022; **28**:2321–8.
- Tarhini AA, Joshi I, Garner F. Sargramostim and immune checkpoint inhibitors: combinatorial therapeutic studies in metastatic melanoma. *Immunotherapy* 2021; **13**:1011–29.
- Pradhan AK, Bhoopathi P, Maji S, Kumar A, Guo C, Mannangatti P, et al. Enhanced cancer therapy using an engineered designer cytokine alone and in combination with an immune checkpoint inhibitor. *Front Oncol* 2022; **12**:812560.
- Mortezaei K, Majidpoor J. Checkpoint inhibitor/interleukin-based combination therapy of cancer. *Cancer Med* 2022; **11**:2934–43.
- Song M, Kim HJ, Kim EY, Shin M, Lee HC, Hong Y, et al. ppGpp-dependent stationary phase induction of genes on *Salmonella* pathogenicity island 1. *J Biol Chem* 2004; **279**:34183–90.
- Trouplin V, Boucherit N, Gorvel L, Conti F, Mottola G, Ghigo E. Bone marrow-derived macrophage production. *J Vis Exp* 2013: e50966.
- Zhang YH, He M, Wang Y, Liao AH. Modulators of the balance between M1 and M2 macrophages during pregnancy. *Front Immunol* 2017; **8**:120.
- Jiang SN, Park SH, Lee HJ, Zheng JH, Kim HS, Bom HS, et al. Engineering of bacteria for the visualization of targeted delivery of a cytolytic anticancer agent. *Mol Ther* 2013; **21**:1985–95.
- Gao J, Liang Y, Wang L. Shaping polarization of tumor-associated macrophages in cancer immunotherapy. *Front Immunol* 2022; **13**:888713.
- Pan Y, Yu Y, Wang X, Zhang T. Tumor-associated macrophages in tumor immunity. *Front Immunol* 2020; **11**:583084.
- Strachan DC, Ruffell B, Oei Y, Bissell MJ, Coussens LM, Pryer N, et al. CSF1R inhibition delays cervical and mammary tumor growth in

- murine models by attenuating the turnover of tumor-associated macrophages and enhancing infiltration by CD8⁺ T cells. *Oncoimmunology* 2013;**2**:e26968.
40. Li Y, Wang R, Gao Q. The roles and targeting of tumor-associated macrophages. *FBL* 2023;**28**:207.
 41. Yonemitsu K, Pan C, Fujiwara Y, Miyasato Y, Shiota T, Yano H, et al. GM-CSF derived from the inflammatory microenvironment potentially enhanced PD-L1 expression on tumor-associated macrophages in human breast cancer. *Sci Rep* 2022;**12**:12007.
 42. Yan WL, Shen KY, Tien CY, Chen YA, Liu SJ. Recent progress in GM-CSF-based cancer immunotherapy. *Immunotherapy* 2017;**9**:347–60.
 43. Stringhini M, Spadafora I, Catalano M, Mock J, Probst P, Spörri R, et al. Cancer therapy in mice using a pure population of CD8⁺ T cell specific to the AH1 tumor rejection antigen. *Cancer Immunol Immunother* 2021;**70**:3183–97.
 44. Gupta KH, Nowicki C, Giurini EF, Marzo AL, Zloza A. Bacterial-based cancer therapy (BBCT): recent advances, current challenges, and future prospects for cancer immunotherapy. *Vaccines (Basel)* 2021;**9**:1497.
 45. Lim D, Kim KS, Kim H, Ko KC, Song JJ, Choi JH, et al. Anti-tumor activity of an immunotoxin (TGF α -PE38) delivered by attenuated *Salmonella typhimurium*. *Oncotarget* 2017;**8**:37550–60.
 46. Gao S, Jung JH, Lin SM, Jang AY, Zhi Y, Bum Ahn K, et al. Development of oxytolerant *Salmonella typhimurium* using radiation mutation technology (RMT) for cancer therapy. *Sci Rep* 2020;**10**:3764.
 47. Kim JE, Phan TX, Nguyen VH, Dinh-Vu HV, Zheng JH, Yun M, et al. *Salmonella typhimurium* suppresses tumor growth via the pro-inflammatory cytokine interleukin-1 β . *Theranostics* 2015;**5**:1328–42.
 48. Na HS, Kim HJ, Lee HC, Hong Y, Rhee JH, Choy HE. Immune response induced by *Salmonella typhimurium* defective in ppGpp synthesis. *Vaccine* 2006;**24**:2027–34.
 49. Jeong JH, Kim K, Lim D, Jeong K, Hong Y, Nguyen VH, et al. Anti-tumoral effect of the mitochondrial target domain of Noxa delivered by an engineered *Salmonella typhimurium*. *PLoS One* 2014;**9**:e80050.
 50. Singh P, Sharma L, Kulothungan SR, Adkar BV, Prajapati RS, Ali PSS, et al. Effect of signal peptide on stability and folding of *Escherichia coli* thioredoxin. *PLoS One* 2013;**8**:e63442.
 51. Guo S, Alshamy I, Hughes KT, Chevance FFV. Analysis of factors that affect FlgM-dependent type III secretion for protein purification with *Salmonella enterica* serovar Typhimurium. *J Bacteriol* 2014;**196**:2333–47.
 52. Han Y, Liu D, Li L. PD-1/PD-L1 pathway: current researches in cancer. *Am J Cancer Res* 2020;**10**:727–42.
 53. Bellucci R, Martin A, Bommarito D, Wang K, Hansen SH, Freeman GJ, et al. Interferon- γ -induced activation of JAK1 and JAK2 suppresses tumor cell susceptibility to NK cells through upregulation of PD-L1 expression. *Oncoimmunology* 2015;**4**:e1008824.
 54. Green ER, Meccas J. Bacterial secretion systems: an overview. *Microbiol Spectr* 2016;**4**:10.
 55. Costa TRD, Felisberto-Rodrigues C, Meir A, Prevost MS, Redzej A, Trokter M, et al. Secretion systems in Gram-negative bacteria: structural and mechanistic insights. *Nat Rev Microbiol* 2015;**13**:343–59.
 56. Singer HM, Erhardt M, Steiner AM, Zhang MM, Yoshikami D, Bulaj G, et al. Selective purification of recombinant neuroactive peptides using the flagellar type III secretion system. *mBio* 2012;**3**:e00115-12.
 57. Reeves AZ, Spears WE, Du J, Tan KY, Wagers AJ, Lesser CF. Engineering *Escherichia coli* into a protein delivery system for mammalian cells. *ACS Synth Biol* 2015;**4**:644–54.
 58. Lim D, Jung WC, Jeong JH, Song M. Targeted delivery of the mitochondrial target domain of Noxa to tumor tissue via synthetic secretion system in *E. coli*. *Front Bioeng Biotechnol* 2020;**8**:840.